Effect of Mixed Acid Fluid on the Pore Structure of High Rank Coal and Acid Fluid Optimization

Chunxia Wang, Jianliang Gao, and Xuebo Zhang*

ACCESS | Metrics & More | Article Recommendations

ABSTRACT: Acidizing technology is an important means to increase production in oil-gas reservoirs. In recent years, acidizing technology has been widely used to increase the permeability of coal seams to enhance gas extraction, where acidizing fluid is the key factor to determine the permeability improvement effect by acidizing technology. In order to clarify the influence of mixed acid fluid on the pore structure of high rank coal and seek the optimal mixed acid fluid suitable for acidizing and permeability improvement of high rank coal in the Jiaozuo coal mine area. Taking the Jiulishan Mine in the Jiaozuo mining area as an example, low field nuclear magnetic resonance (LFNMR) test and static dissolution test were conducted to obtain the T_2 spectrum, porosity, movable fluid saturation, pore throat distribution, nuclear magnetic permeability, and dissolution rate of coal samples before and after treatment with distilled water and three mixed acid fluids. On this basis, the influence of mixed acid fluid on the pore structure of high rank coal was analyzed and the optimal mixed acid fluid suitable for high rank coal was

selected. The results showed that the pore size, number, and volume of all kinds of pore sizes of coal samples treated with distilled water all decreased, which was manifested by the decrease of effective porosity and nuclear magnetic permeability. After acidification, the proportion of micropore volume in coal decreased significantly, the number and proportion of pore volume of mesopores and macropore-microfractures increased significantly, and the connectivity between mesopores and macropore-microfractures was enhanced, which was characterized by the increase in effective porosity and nuclear magnetic permeability of coal samples. After acidification, the pore-throat ratio of adsorption pores of all coal samples decreased, while the pore-throat ratio of seepage pores increased. By comparatively analyzing the change law of pore structure of coal samples before and after acidizing with three kinds of mixed acid fluids, the optimal mixed acid fluid suitable for acidizing and permeability improvement of high rank coal in the Jiaozuo coal mine area was selected, which was 12%HCL +3%HF.
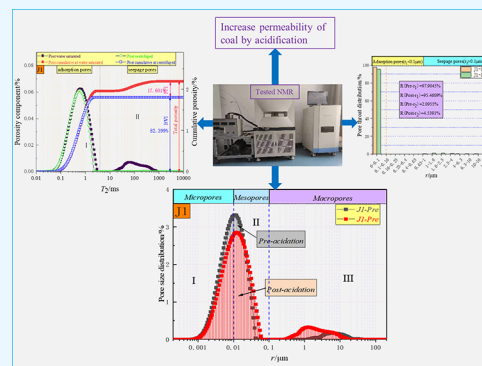
1. INTRODUCTION

Coalbed methane, a highly efficient clean energy with abundant reserves in China, is not only a disastrous gas that causes gas accidents in coal mines but also an unconventional natural gas that exists in coal holes and fissures in adsorption and free states.[1] Gas extraction is an effective way to prevent gas accidents and develop coal bed methane. However, the gas extraction is restricted due to low porosity and low permeability of coal reservoirs in China.[2] Studies have shown that the permeability of coal seam directly determines the difficulty in gas extraction.[3−5] How to improve the permeability of low-permeability coal bed is the key problem to strengthen gas extraction and prevent gas disaster. The pore-fissure system in coal is the main channel for gas flow,[6] so the microscopic pore structure of coal is an important factor determining its permeability.[7−11] In essence, the factors affecting coal permeability mainly affect penetrability through affecting the micropore structure of coal. Therefore, adopting effective technical means to improve the pore structure of coal

bed and increase its permeability is the key to improve the gas extraction rate.

At present, hydraulic fracturing technology has been widely used in gas extraction owing to its capacity of placing the coal body under huge pressure to produce a large number of cracks and thus increase the permeability of coal bed. However, fracturing the fluid residue and filtrate will block pores and fractures after hydraulic fracturing.[12] Clay minerals in coal, such as kaolinite, montmorillonite, illite, chlorite, etc., will expand when they meet water,[13] leading to a great decrease in permeability of coal. It can be seen that hydraulic fracturing will cause damage to coal bed to a certain extent,[14] limiting its

large-scale application in gas extraction. Domestic and foreign scholars have found that there are many kinds of inorganic minerals in coal bed fractures, among which carbonate, clay, quartz, feldspar, and sulfide[15] are common minerals. Some minerals are embedded in the coal matrix, while some minerals are filled in the cracks of coal,[16] occupying the pore and fissure space and blocking the fissures and pore throats. Although the mineral content in the coal is not high because the pores and microfissures in the coal are very small, the minimal mineral filling will cause a great reduction of the pore space, thus hindering the fluid flow and greatly reducing the permeability of the coal seam. Based on the understanding of chemical reactions, acid fluid can dissolve the minerals filling in the cracks and pores of coal.[17,18] In recent years, many experts and scholars have paid attention to the acidification technology, that is, increasing the permeability of coal bed by injecting acid fluid into coal bed and corroding minerals filled in coal fractures. Researchers have carried out a lot of research studies on the influence of acidification on the pore structure and permeability of coal. Zhang et al.[19] studied the effects of HCL and HNO_3 on the microcrystalline structure and micropore structure of high-sulfur coal and found that the combined use of HCL and HNO_3 increased the specific surface area and micropore of coal. Yang et al.[20] studied the influence of acetic acid dissolution time on phase evolution and surface morphology of coal. Yu et al.[21] studied the effect of acetic acid concentration on the functional groups and microcrystalline structure of bituminous coal. Xie et al.[22] and Ni et al.[23] added surfactant sodium dodecyl sulfate (SDS) into the mixed solution of hydrochloric acid and hydrofluoric acid to study the effects of SDS synergistic acidification on fractal characteristics and pore-fracture changes of coal pores. The results showed that after SDS synergistic acidification, the proportion of seepage pore volume increased by 5.99%, the acidizing effect of HCL and HF on coal was enhanced, the porosity of coal was increased, and the connectivity between the large pore and fracture was increased. Balucan et al.[24] studied the influence of HCl and HF on the permeability and compressibility of coal under different effective stresses. The results showed that HF treatment caused more mineral alteration and produced new crystal minerals. When the effective stress increased, the newly produced crystal minerals supported fractures and improved permeability. Balucan et al.[25] found through X-ray μCT study that hydrochloric acid acidification could improve fluid flow channels for calcite-filled cleats. Ni et al. and Balucan et al. only studied the acidification effect of the mixed acid of hydrochloric acid and hydrofluoric acid on low-rank coal but did not study the acidification effect of the mixed acid of hydrochloric acid and hydrofluoric acid on medium and high-rank coal.[23,24] This paper focuses on the influence of the mixed acid on the pore structure and permeability of high-rank coal in the Jiulishan coal mine, so as to select the optimal acid system suitable for high-rank coal in the Jiulishan coal mine. Ramandi et al.[26] obtained the structures of syngenetic minerals and secondary minerals by micro-CT scanning and studied the dissolution effects of syngenetic minerals and secondary minerals on the porosity and permeability of coal using the finite volume method. The results showed that the dissolution effect of minerals increased the porosity and permeability of coal, thus improving the gas extraction rate.

In conclusion, acidizing technology can effectively improve the pore structure of coal and the permeability of coal bed, and acid fluid is the key factor determining the effect of acidification and permeability improvement. Most of the existing research literature focuses on using the mud acid that is widely used in oilfield stimulation as acidizing fluid to analyze the permeability improvement effect on low rank coal by acidification. However, the geological characteristics and mineral composition of coal reservoir, carbonate reservoir, and sandstone reservoir are very different, so the mixed acid fluid suitable for coal reservoir acidification is yet to be determined. In existing studies, the comparative analysis of the influence of different types of mixed acid fluids on the pore structure of high rank coal has not been reported. Therefore, finding the optimal mixed acid fluid suitable for acidizing and permeability improvement of high rank coal is a key link to increase coal permeability by acidizing technology. In order to clarify the effect of mixed acid fluid on the pore structure of high-rank coal and seek the optimal mixed acid fluid for acidification and permeability improvement of high-rank coal in the Jiaozuo coal mine area, a low-field nuclear magnetic resonance (LFNMR) test and static dissolution test were carried out to study the effects of different mixed acid fluids on the pore structure of high-rank coal. Nuclear magnetic resonance (NMR), as a non-destructive, rapid, and accurate method of pore structure measurement, has been widely used in the pore structure measurement of coal samples in recent years. Nuclear magnetic resonance experiment can obtain the quantity and distribution state of liquid in the coal sample by measuring the relaxation characteristics of water or other fluid protons, so as to obtain the change rule of the pore structure of the coal sample. In this paper, taking the Jiulishan coal mine in the Jiaozuo mining area as an example, the coal pillars and coal particles were soaked with distilled water and three kinds of mixed acid fluids (8% HCl +7%HBF_4, 12%H_3PO_4 + 3%HF, and 12%HCl +3%HF), which are commonly used in oil fields for oilfield stimulation. The porosity, permeability, pore throat distribution, and dissolution rate of coal samples treated with distilled water and three kinds of mixed acid fluids were measured by a low-field nuclear magnetic resonance test and static dissolution test. The influence of mixed acid fluid on the pore structure of high rank coal was studied by analyzing the variation law of each parameter, and the optimal mixed acid fluid suitable for high rank coal was selected. This study provides experimental support and theoretical basis for promoting the application of acidification technology in coal bed.

2. EXPERIMENTAL PRINCIPLE AND SCHEME

2.1. Experimental Principle. *2.1.1. Low-Field NMR Test Principle.* Low-field nuclear magnetic resonance (LFNMR) technology is when the spin magnetic moment of a ^{1}H nucleus in fluid under the condition of extremely low magnetic field intensity is changed after being affected by the external magnetic field and then gradually returns to its initial state when the external magnetic field is withdrawn. The number of hydrogen atoms in the fluid can be determined by the relationship between the NMR signal intensity distribution (T_2 spectrum) and the transverse relaxation time. The number, size, and location of T_2 spectrum peaks in NMR can be used to analyze the pore structure of coal, including pore type, size, and distribution, as well as the connectivity between pores and fractures. The relationship between the transverse relaxation time and pore radius can be expressed as follows:

$$\frac{1}{T_2} = \rho \left(\frac{S}{V} \right)_{pore} = F_s \frac{\rho}{r} \tag{1}$$

$$r = CT_2 \tag{2}$$

where T_2 is the transverse relaxation time (ms), ρ is the transverse surface relaxation strength (μm/ms), of which the value depends on the mineral composition of the pore surface and the hydrogen-containing nature of the fluid in the pore, and S and V represent the pore surface area (μm^2) and pore volume (μm^3), respectively. F_s is the pore shape factor (spherical pore, F_s = 3; columnar pore, F_s = 2), r is the pore radius (μm), and C is the pore conversion coefficient (μm/ms),[6] which is a constant related to pore surface relaxation.

According to eq 2, the pore size is proportional to the T_2 value of transverse relaxation time. In the T_2 spectrum distribution curve, different T_2 values correspond to different pore sizes: for a certain core, as the conversion coefficient is constant, the longer the abscissa relaxation time T_2 is, the larger the pore radius is, the shorter the relaxation time T_2 is, and the smaller the pore radius is. In contrast, the amplitude of the T_2 spectrum reflects the number of pores. The higher the amplitude of ordinate signal is, the more pores there are under the corresponding pore radius, indicating that the pores in the coal are better developed. The continuity of T_2 spectrum signals reflects the connectivity of the microscopic pore structure. The area bounded by each peak in the T_2 spectrum distribution and the transverse relaxation time axis, namely, the T_2 spectral area, represents the nuclear magnetic porosity.

The nuclear magnetic permeability of coal samples cannot be measured directly by LFNMR technology but is characterized indirectly by relaxation parameters and theoretical models. At present, the commonly used method is to use the Coates model to calculate the nuclear magnetic permeability on the basis of the porosity and movable fluid saturation of coal samples measured by LFNMR. The mathematical expression of the Coates model is as follows:

$$K = \left(\frac{\varphi}{C} \right)^4 \left(\frac{FFI}{BVI} \right)^2 \tag{3}$$

where K is the nuclear magnetic permeability, φ is the nuclear magnetic porosity, %; C is the regional empirical value coefficient, FFI is the movable fluid saturation, %; and BVI is the bound fluid saturation, %.

2.1.2. Principle of Static Dissolution Experiment. The dissolution of acid to rock, expressed by the dissolution rate, is characterized by the actual amount of rock dissolved. The dissolution rate is the change rate of coal mass per unit mass before and after the reaction with acid at a certain temperature. The dissolution rate determines the acidizing effect, so the dissolution ability of acid to the coal sample can be measured by using the dissolution rate. The calculation formula of the dissolution rate R_c is as follows:

$$R_c = \frac{m_1 - (m_2 - m_3)}{m_1} \tag{4}$$

where R_c is the dissolution rate, %; m_1 is the initial mass of the coal sample before acidification treatment, g; m_2 is the mass of the coal sample containing filter paper after acidification treatment, g; and m_3 is the mass of dry filter paper, g.

2.1.3. Principle of Acidification. The principle of coal bed acidification is to inject one or several kinds of acid fluids into the coal bed, use acid fluid to dissolute the minerals in the pores and cracks of the coal bed, and improve the flow conductivity of cracks in the coal bed so as to improve the permeability of the coal bed and achieve the purpose of strengthening the gas extraction. Therefore, the mineral composition in coal and the chemical reaction characteristics between minerals with acid fluids are the basis for the selection of the optimal acid fluid and the implementation of acidizing-based permeability improvement technology.

In order to determine the mineral composition and content of the Jiulishan coal mine, an X-ray diffractometer (XRD, produced by Japan Rigaku Co., Cu target, output power 9 KW) was used to test the original coal samples, with a test angle of 0−70° and a test speed of 5 °/min. Jade 6.0 software was used to retrieve the XRD test results and make quantitative analysis. It was concluded that the minerals in the Jiulishan coal mine mainly include quartz 50.9%, calcite 21.4%, barite 13.6%, kaolinite 10.2%, ankerite 2.0%, and chlorite 1.9%. The XRD diffraction pattern of original coal samples in the Jiulishan coal mine is shown in Figure 1.
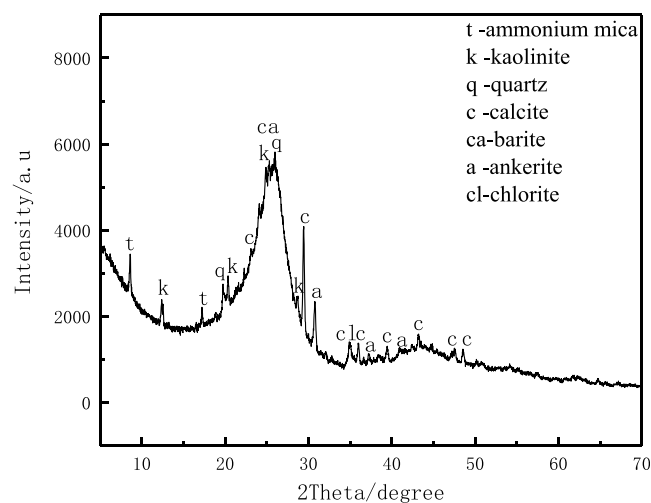

Figure 1. XRD diffraction pattern.

Figure 1 shows that the Jiulishan coal mine also contains a small amount of ammonium mica, which cannot be quantitatively analyzed due to its extremely low content. combined with XRD quantitative analysis results, the coal in the Jiulishan coal mine contains calcite, ankerite, and other carbonate minerals, which are easy to be dissolved by acid. The main chemical reaction equations involved in acidizing the coal sample from the Jiulishan coal mine are as follows:
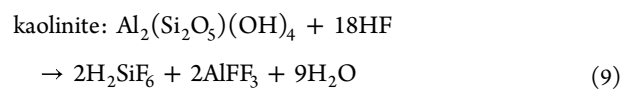
$$\text{calcite: } CaCO_3 + 2H^+ \rightarrow Ca^{2+} + CO_2 \uparrow + H_2O \tag{5}$$

$$\text{ankerite: } CaMg(CO_3)_2 + 4H^+$$
$$\rightarrow Ca^{2+} + Mg^{2+} + 2CO_2 \uparrow + 2H_2O \tag{6}$$

$$CaFe(CO_3)_2 + 4H^+ \rightarrow Ca^{2+} + Fe^{2+} + 2CO_2 \uparrow + 2H_2O \tag{7}$$

$$\text{quartz: } SiO_2 + 6HF \rightarrow H_2SiF_6 + 2H_2O \tag{8}$$

$$\text{kaolinite: } Al_2(Si_2O_5)(OH)_4 + 18HF$$
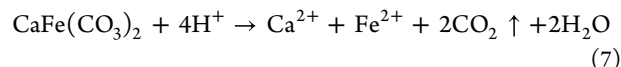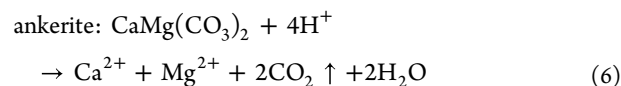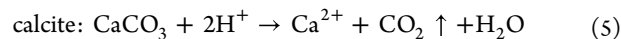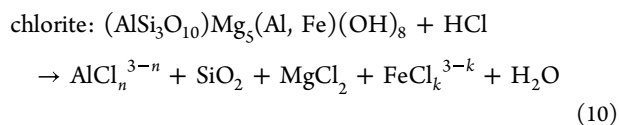$$\rightarrow 2H_2SiF_6 + 2AlF_3 + 9H_2O \tag{9}$$

Table 1. Vitrinite Reflectance and Maceral and Proximate Analyses of the Coal Sample (%)[a]

coal sample	$R_{o,max}$	maceral content				proximate analysis			
		V	I	E	MM	M_{ad}	A_{ad}	V_{ad}	F_{cad}
Jiulishan coal mine	2.59	78.3	14.1	0	7.6	3.15	8.24	6.3	82.31

[a]$R_{o,max}$ represents the maximum vitrinite reflectance; V represents vitrinite; I represents inertinite; E represents exinite; MM represents mineral; M_{ad} represents the moisture content of air dried basis; A_{ad} represents the ash content of air dried basis; V_{ad} represents volatiles; and F_{cad} represents the carbon content of air dried basis.

chlorite: $(AlSi_3O_{10})Mg_5(Al, Fe)(OH)_8 + HCl$

$$\rightarrow AlCl_n^{3-n} + SiO_2 + MgCl_2 + FeCl_k^{3-k} + H_2O \tag{10}$$

Kaolinite and chlorite are aluminosilicate clay minerals, which do not react completely with hydrochloric acid. Barite is chemically stable, which is insoluble in water, hydrochloric acid, and hydrofluoric acid.

2.2. Materials and Methods. *2.2.1. Preparation of Coal Samples.* The experimental coal samples used in this paper are collected from the mining face of the no. 15 mining area of the Jiulishan Coal Mine of Jiaozhuo Coal Energy Co., Ltd. of Henan Province. The maximum vitrinite reflectance and maceral and proximate analysis results of coal are shown in Table 1. According to Table 1, the maximum vitrinite reflectance of coal is 2.59%, which belongs to anthracite. Two kinds of coal samples were prepared in strict accordance with the "Method for Preparation of Coal Samples" (GB/T 474-2008 (China)). The coal core with a diameter of $\varphi 25 \times 50$ mm was drilled by a core drilling machine, which was used for the low field nuclear magnetic resonance test to analyze the effect of mixed acid fluid on the pore structure of coal. The coal samples were broken into coal particles with diameters of 3−6 mm, which were used for static dissolution experiment to analyze the dissolution ability of mixed acid fluid on coal.

2.2.2. Acid Preparation and Acid Leaching Experiment. According to the existing commercially available concentration of 38% hydrochloric acid (HCL), 85% of phosphoric acid (H_3PO_4), 40% of hydrofluoric acid (HF), 40% of fluoroboric acid (HBF_4), distilled water, four sets of solutions were prepared. They were liquid used for hydraulic fracturing or coal seam water injection (distilled water), and three acid systems commonly used in oil fields with a good production stimulation effect were a mixed solution of hydrochloric acid and fluoroboric acid (8%HCL + 7%HBF$_4$), mixed solution of phosphoric acid and hydrofluoric acid (12%H$_3$PO$_4$ + 3%HF), and mixed solution of hydrochloric acid and hydrofluoric acid (12%HCL + 3%HF); the total concentration of the mixed acid was 15%. The four solutions are referred to as acid 0, acid 1, acid 2, and acid 3. Among them, hydrochloric acid and phosphoric acid are strong acids, which can dissolve carbonate minerals such as calcite and dolomite in coal. Hydrofluoric acid and fluoroborate acid can react with aluminosilicate such as silica and kaolinite in coal. Since the acid is volatile and hydrofluoric acid is highly corrosive to glass containers made of various silicon-containing materials, the prepared acids were stored in sealed inert plastic bottles.

Acid 0, acid 1, acid 2, and acid 3, each of which was 300 mL in volume, were prepared and stored in sealed inert plastic bottles. The four coal cores prepared from the Jiulishan coal mine were marked as J0, J1, J2, and J3. They were soaked in inert plastic bottles containing four kinds of acid fluids and sealed according to the one-to-one correspondence principle of

numbers, and then placed in a constant temperature water bath for reaction at 30 °C for 24 h. Acid 0, acid 1, acid 2, and acid 3 were prepared at a solid−liquid ratio of 1 g:50 mL and stored in sealed inert plastic bottles for later use.

2.3. Experimental Process. *2.3.1. LFNMR Experimental Process.* ① First, the coal samples before treatment were put into a thermostatic drying oven and dried at 80 °C for 48 h, followed by cooling to room temperature and weighing the mass of each dry coal sample by a balance. ② The dried coal samples were put into a vacuum water saturation device containing distilled water for 24 h. ③ The mass, length, and diameter of each coal sample in the saturated state were measured, and the volume was calculated. ④ LFNMR experiment was performed on each coal sample before acidification to test the distributions of the T_2 spectrum and pore size. ⑤ Then, centrifugal treatment was conducted to reach a perfect irreducible water condition (centrifuge pressure and time were 200 Psi and 1.5),[27] and the mass of each coal sample in the centrifugal state was weighed. ⑥ LFNMR experiment was carried out on the coal samples after centrifugation to test the T_2 spectral distribution and pore size distribution. ⑦ All coal samples were dried and acidified using the method described in Section 2.2.2. ⑧ The treated coal samples were placed into a thermostatic drying oven and dried for 48 h at 80 °C before cooling to room temperature, and then the mass of each dry coal sample was weighed with a balance. Steps ②−⑥ were repeated to study the influence of the four solutions on the pore structure of coal samples. Detailed experimental steps are shown in Figure 2.

2.3.2. Static Dissolution Test Process. ① Coal particles (15 g) with a diameter of 3−6 mm were weighed with a precision balance of 1/10,000 and put into a constant temperature drying oven at 80 °C for 12 h. ② After cooling to room
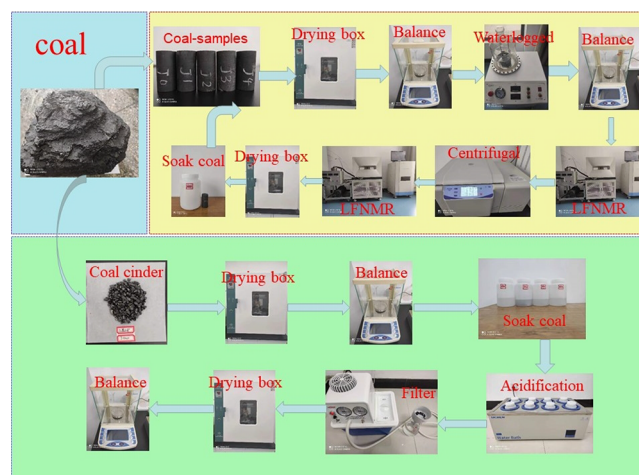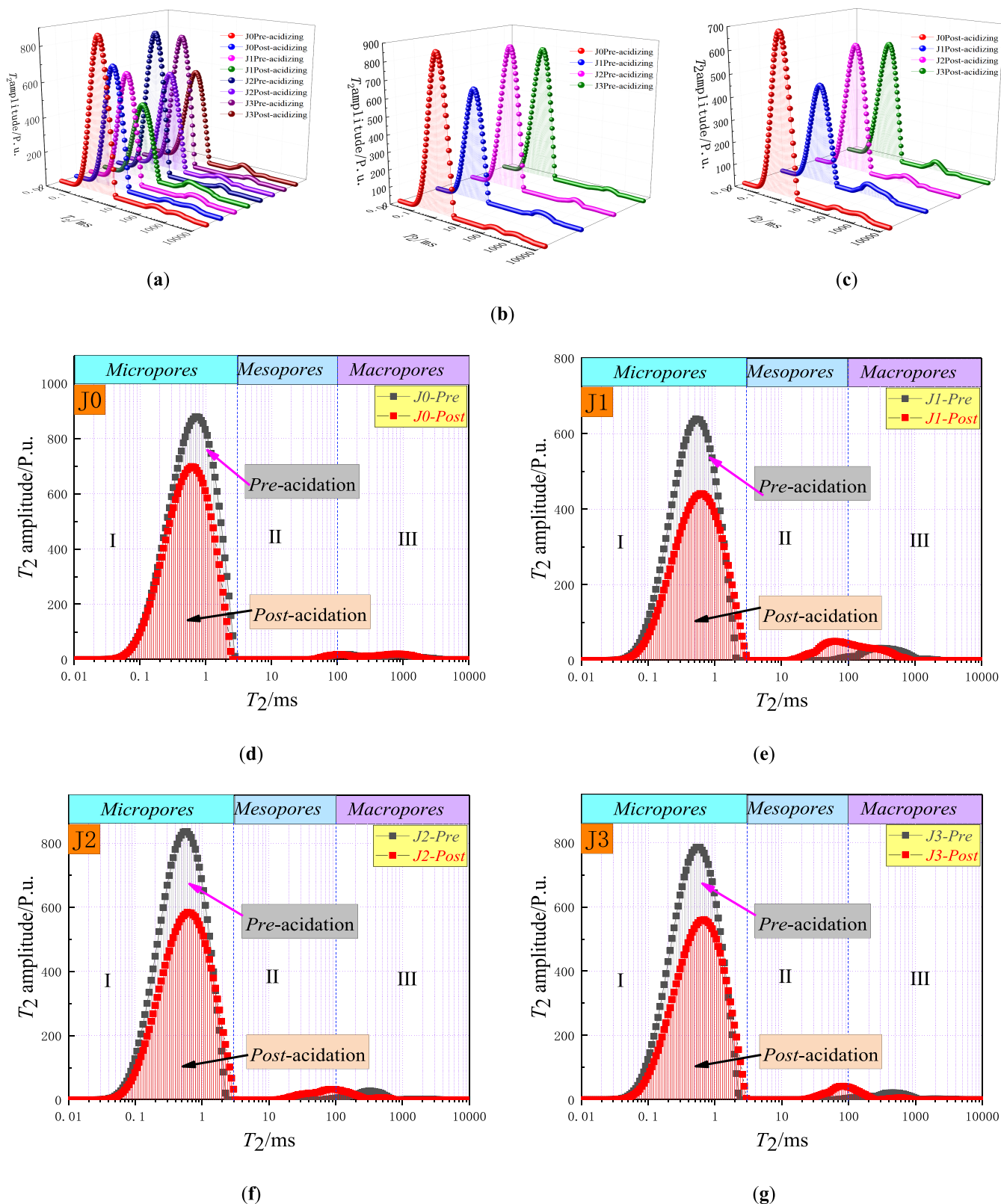

Figure 2. Schematic diagram of the experimental equipment and process.

Figure 3. (a) Comparison of T_2 spectra before and after treatment of four kinds of acid solutions; (b) comparison of T_2 spectra before treatment of four kinds of acid solutions; (c) comparison of T_2 spectra after treatment of four kinds of acid solutions; (d) comparison of T_2 spectra before and after treatment of acid 0; (e) comparison of T_2 spectra before and after treatment of acid 1; (f) comparison of T_2 spectra before and after treatment of acid 2; (g) comparison of T_2 spectra before and after treatment of acid 3.

temperature, four coal samples (3 g/part) were weighed from the dry coal particles and denoted as J0, J1, J2, and J3. ③ The weighed coal particles were poured into the inert plastic bottles

storing four kinds of solutions described in 2.2.2 according to the one-to-one correspondence principle of numbers, sealed, and placed into a constant temperature water bath for reaction

at 30 °C for 12 h. ④ Using a circulating water multi-purpose vacuum pump, the acid-leached coal samples were rinsed and filtered repeatedly with distilled water in a Bouchard funnel until the pH value was neutral. ⑤ The filtered coal sample was placed together with filter paper into a constant temperature drying oven for drying at 80 °C for 24 h until the coal sample reached a constant weight. ⑥ After cooling to room temperature, the mass of dry coal sample together with filter paper was weighed by a 1/10,000 precision balance. ⑦ The dissolution rate of the acidified coal sample was calculated. The dissolution effects of four kinds of solutions on the coal sample were studied. Detailed experimental steps are shown in Figure 2.

2.4. Experimental Instrument. The experimental instrument used in this paper is the Meso-MR23-060H-I low-field NMR tester (Figure 2) produced by Suzhou NIUMAG Analytical Instrument Corporation. Experimental conditions are as follows: magnetic field intensity is 0.5 T, ^{1}H atomic resonance frequency and radio frequency pulse frequency are 21.67mhz, and the temperature of the magnet is controlled at 32 ± 0.1 °C.

3. RESULTS

3.1. Analysis of T_2 Spectrum Results. According to the principle of the LFNMR test, the location of the T_2 spectrum peak on the relaxation time axis is proportional to pore size, the T_2 spectrum peak is proportional to the number of pores with the corresponding pore size, and the increase of T_2 amplitude indicates the increase of the number of pores.[28] Therefore, according to the peak position, peak number, peak shape, and amplitude of the T_2 spectrum of the coal core in the saturated state, the pore structure of coal can be analyzed qualitatively and quickly. T_2 spectrum curves of saturated coal samples before and after treatment with four solutions are shown in Figure 3. Before acidification, the four coal samples all show three peaks. According to eq 2 and the pore classification method proposed by Yao and Liu,[29] peak I ($T_2 < 2.5$ ms) on the left side corresponds to the micropore, peak II(2.5 ~ 100 ms) in the middle corresponds to the mesopore, and peak III ($T_2 > 100$ ms) corresponds to the macropore-microcrack. The areas enclosed by the T_2 spectra at zones I, II, and III and the transverse relaxation time axis represent the volumes of micropore, mesopore, and macropore-microcrack of coal samples.[23,30] It can be seen from Figure 3 that the peak I value of the micropore was the highest, but peak I existed independently from peak II and peak III, indicating that the pore volume proportion of the micropore was the largest and the micropore was developed most significantly, but the connectivity between the micropore and mesopore and that between the micropore and macropore-microcrack were poor. The peak values of the mesopore and macropore-microcrack were relatively low, while the peak valley between the mesopore peak and macropore-microcrack peak was relatively flat, indicating that the volume proportion of the mesopore and macropore-microcrack was relatively low, the mesopore and macropore-microcrack were relatively developed, and the connectivity between the mesopore and macropore-microcrack was good. After acidification, the T_2 spectral distribution curves of J1, J2, and J3 treated with three kinds of mixed acid fluids all showed three spectral peaks. The peak value of peak I representing the micropore was significantly lower than that before acidification; the right side of the spectral peak shifted to the right; and the peak area was decreased, indicating that

the pore size developed to a mesopore and macropore, and the volume proportion of micropores decreased significantly. After acidification, the peak values of peak II representing the mesopore and peak III representing the macropore-microcrack increased significantly, the peak area increased and the peak range was widened, and the peak valley between the mesopore and macropore-microcrack became more flat, indicating the enhancement of continuity between the mesopore and macropore-microcrack. The results indicate that the number and volume proportion of the mesopore and macropore-microcrack both increased significantly after acidification, in which the number of mesopore and macropore-microcrack increased most significantly, and the connectivity between the mesopore and macropore-microcrack increased, which is consistent with the conclusion drawn in the literature.[31] In contrast, the T_2 spectral distribution curve of the J0 coal sample treated by distilled water shifted to the left as a whole, in which peak I shifted the most significant, and the amplitudes of all three peaks decreased, indicating that the pores of coal samples treated with distilled water evolved from a micropore to a smaller micropore, and the pore size, number, and volume of the micropore, mesopore, and macropore-microcrack in coal samples treated with distilled water all decreased. This may be because there were water-sensitive clay minerals in the pore-fissure of coal, which expanded when they met water, occupying the position of the primary pore-fissure, causing some mesopores and macropores to turn into micropores, or even blocking the pore-throat and sealing the micropores, resulting in the reduction of the pore size, pore number, and pore volume of the coal sample. To this end, the mixed acid fluids dissolved the minerals in the pore fissures of coal, enlarged the space of the pore fissures, and dredged the originally blocked pore-fissures, making the new fissures connect with the original fissures, which increased the connectivity between the coal pore fissures and made some micropores become mesopores and macropores. Therefore, the volume proportion of micropores decreased after acidification, while that of mesopores and macropores increased.

By comparing the T_2 spectrum distribution curves of the three coal samples after acidification, it can be seen that compared with coal sample J2 acidified by 12%H_3PO_4 + 3% HF, the peak amplitude and spectrum area of peak II representing the mesopore and peak III representing the macropore-microcrack in the T_2 spectrum of J1 and J3 acidified by 8%HCL + 7%HBF_4 and 12%HCL + 3%HF were significantly increased. This indicates that compared with J2 after acidification, the pore number and pore volume of the mesopore and macropore-microcrack of J1 and J3 after acidification increased more significantly, and the connectivity between pores was improved, which is due to fact that the dissolution effect of 8%HCL + 7%HBF_4 and 12%HCL + 3% HF on minerals in coal fissures is stronger than 12%H_3PO_4 + 3%HF. The results indicate that the mixed acid fluids of 8% HCL + 7%HBF_4 and 12%HCL + 3%HF can better dissolve the minerals filled in the coal pore fissures than 12%H_3PO_4 + 3% HF, leading to a greater increase in the number and volume of coal fissures, so that acidification can play a better role in hole opening and expanding, and the connectivity between coal fissures can be enhanced to a greater extent, which is more conducive to the production and transport of gas from the coal fissures. Therefore, 8%HCL + 7%HBF_4 or 12%HCL + 3%HF is more suitable than 12%H_3PO_4 + 3%HF for the acidification

and permeability improvement of high rank coal in the Jiaozuo coal mine area.

3.2. Analysis of Changes in Porosity and Movable Fluid Saturation.
3.2.1. Changes in Porosity. The porosity of coal is an important index to characterize the gas storage capacity and structure of coal. NMR-based coal core analysis can measure porosity of coal quickly and accurately. NMR porosity measurement is to establish a porosity characterization model of the correlation between NMR signal intensity and porosity based on standard oil samples with known porosity, then measure the porosity of the coal sample by measuring its nuclear magnetic signal intensity using such model, and finally obtain the corresponding porosity parameters.[32] Nuclear magnetic porosity is determined by the total amount of nuclear magnetic signal. The porosity characterization model established in this paper is shown in Figure 4.
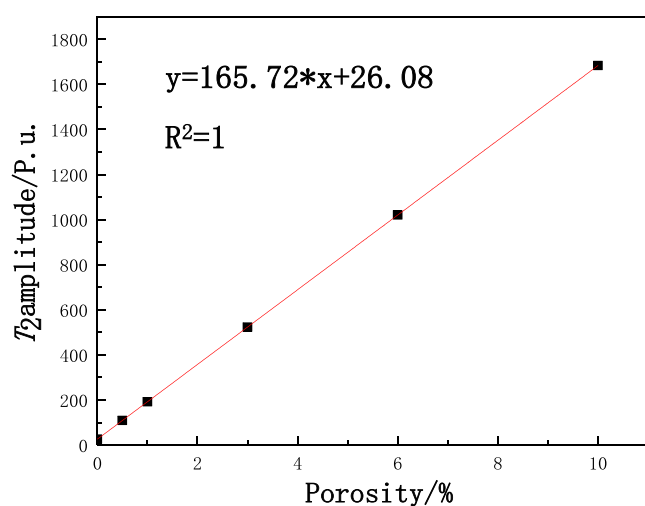

$$y = 165.72 * x + 26.08$$

$$R^2 = 1$$

Figure 4. Porosity model.

Through LFNMR tests on saturated and centrifugal coal samples before and after treatment by four kinds of acid solutions, the saturated porosity and centrifugal porosity of four coal samples before and after acidification were obtained. Saturated porosity is calibrated as total porosity (φ), while centrifugal porosity is calibrated as residual water (bound fluid) porosity ($\varphi 1$), and the difference between the two is effective (movable fluid) porosity ($\varphi 2$).[33] Effective porosity is the portion of porosity with good connectivity that facilitates the flow of movable fluid, which is an important index to evaluate the seepage capacity of coal bed. The higher the effective porosity is, the better the seepage capacity of coal bed is. LFNMR porosity measurement results of coal samples before and after acidification treatment are shown in Table 2.

Table 2 shows that the total porosity and effective porosity of coal sample J0 after distilled water treatment decreased, the effective porosity decreased from 0.22% to 0.14%, and the absolute value of effective porosity decreased by 0.08%, with a decrease rate of 34.88%. This indicates that the total pore volume of the coal sample decreased after distilled water treatment and the connectivity between pores deteriorated as well, which is consistent with the conclusion of the T_2 spectrum analysis above. This indicates that the improper application of hydraulic fracturing or water injection technology in the coal bed may lead to the reduction of effective porosity of the coal bed, thus reducing the permeability of coal and hindering gas extraction.

In contrast to the decrease of effective porosity caused by the treatment with distilled water, the total porosity of J1, J2, and J3 treated with three acid solutions all decreased, while the effective porosity increased, indicating that the total pore volume of the coal samples decreased after acidification, while the connectivity between pores increased. According to previous studies, the connectivity between micropores in coal was extremely poor, and the connectivity between pores was mainly determined by the mesopore and macropore-microcrack. According to the above T_2 spectrum analysis, the volume proportion of the micropore in the original coal sample was relatively high, while that of the mesopore and macropore-microcrack was relatively low. After acidification, the volume of the micropore decreased, while that of the mesopore and macropore-microcrack increased. Due to the dominant position of the micropore in the original coal sample, the increase of volume of the mesopore and macropore-microcrack was less significant than the decrease of volume of the micropore, resulting in the decrease of total porosity and the increase of effective porosity. Effective porosity is an important parameter affecting gas flow in the coal bed. The increase of effective porosity reflects the improvement of gas permeability of the coal bed. The greater the increase of effective porosity is, the better the effect of acidification and permeability improvement is, and the more favorable it is for gas production and transport in the coal bed.

In order to select the optimal mixed acid fluid suitable for acidizing and permeability improvement of high-rank coal in the Jiulishan Coal mine of the Jiaozuo mining area, the effective porosity of coal samples treated with three acid fluids was comparatively analyzed. It can be seen from Table 2 that the effective porosity of coal samples after treatment with the three mixed acid fluids was improved to varying degrees. The effective porosity of coal samples J1, J2, and J3 after acidification increased from 0.26, 0.22, and 0.12% to 0.39, 0.32, and 0.34%, with increase rates of 0.13, 0.104, and 0.22% and increased amplitudes of 49.03, 47.27, and 185.00%, respectively. From the increased amplitude of effective porosity of coal samples after acidification, the effective porosity of J3

Table 2. Porosity Measurement Results (%)

no. of coal sample	before treatment			after treatment			absolute change in effective porosity	relative change in effective porosity
	accumulation of saturated porosity	accumulation of centrifugal porosity	effective porosity	accumulation of saturated porosity	accumulation of centrifugal porosity	effective porosity		
J0	3.63	3.42	0.22	2.88	2.74	0.14	−0.08	−34.88
J1	2.47	2.21	0.26	2.19	1.81	0.39	0.13	49.03
J2	3.20	2.98	0.22	2.65	2.33	0.32	0.10	47.27
J3	3.02	2.90	0.12	2.48	2.14	0.34	0.22	185.00

treated with 12%HCL + 3%HF mixed acid fluid increased the most, indicating that 12%HCL + 3%HF as a mixed acid fluid had the strongest ability to improve the pore structure of high-rank coal in the Jiulishan coal mine of the Jiaozuo mining area and exhibited the best acidification and permeability improvement effects, which is consistent with the conclusion of the above analysis of the T_2 spectrum distribution curve.

In order to further illustrate the superiority of the acidizing method in this paper, the author compared the improvement rate of effective porosity of coal samples after acidizing with 12%HCl + 3%HF mixed acid solution with the research results of domestic researchers, and the results are shown in Table 3.

Table 3. Comparison of Effective Porosity Improvement Rate of Coal after Acidification

source of coal sample	information of acid treatment	improvement rate of effective porosity	researcher
Jincheng mining area, Shanxi	14%HCl + 2% NH₄Cl	100.67%	Li et al.[34]
Jincheng mining area, Shanxi	15%HCl	10.09%	Zhao et al.[35]
Jiangjiahe mine in Xianyang, Shaanxi	12%HCl + 3% HF + 2% NH₄Cl	49.60%	Li et al.[31]
Jiulishan mine in Jiaozuo, Henan province	12%HCl + 3% HF	185%	author of this article

According to the comparison results of effective porosity improvement rate in Table 3, it can be fully demonstrated that the application of 12%HCl + 3%HF mixed acid in acidizing high-rank coal in the Jiulishan coal mine has absolute advantages.

As is known to all, if the dissolution effect of acidification results in the increase of pore volume of coal samples and the enhancement of connectivity between pores, the mass of coal samples in the dry state will decrease, but the moisture content in coal samples in the saturated state will increase. Therefore, it is possible to study the influence of acidification on the pore volume of coal samples by analyzing the mass change of the coal sample in dry and saturated states before and after acidification treatment. In order to verify the accuracy of porosity results measured by LFNMR, a one-thousandth precision balance was used to weigh the mass of three coal cores in the dry state and saturated state before and after soaking in three mixed acid fluids, and the results are shown in Table 4.

It can be seen from Table 4 that compared with the mass of dry coal samples before acidification, the mass of dry coal samples after acidification decreased, indicating that there were substances removed from the coal after acidification; compared with the water content in saturated coal samples before

acidification, the water content in saturated coal samples after acidification increased, indicating that the pore volume of the coal after acidification increased and the connectivity between pores was enhanced. This may be because the acid dissolved the minerals in the coal cracks, generating soluble substances discharged from the coal, expanding the space of coal cracks, strengthening the connectivity between coal cracks, and increasing the mass of water entering the cracks of the coal sample in the saturated state after acidification. Therefore, the mass change rule of coal samples in the dry state and saturated state before and after acidification treatment verifies the NMR test conclusion that the pore volume and effective porosity of mesopores and macropore-microcrack of coal samples after acidification are increased after acidification.
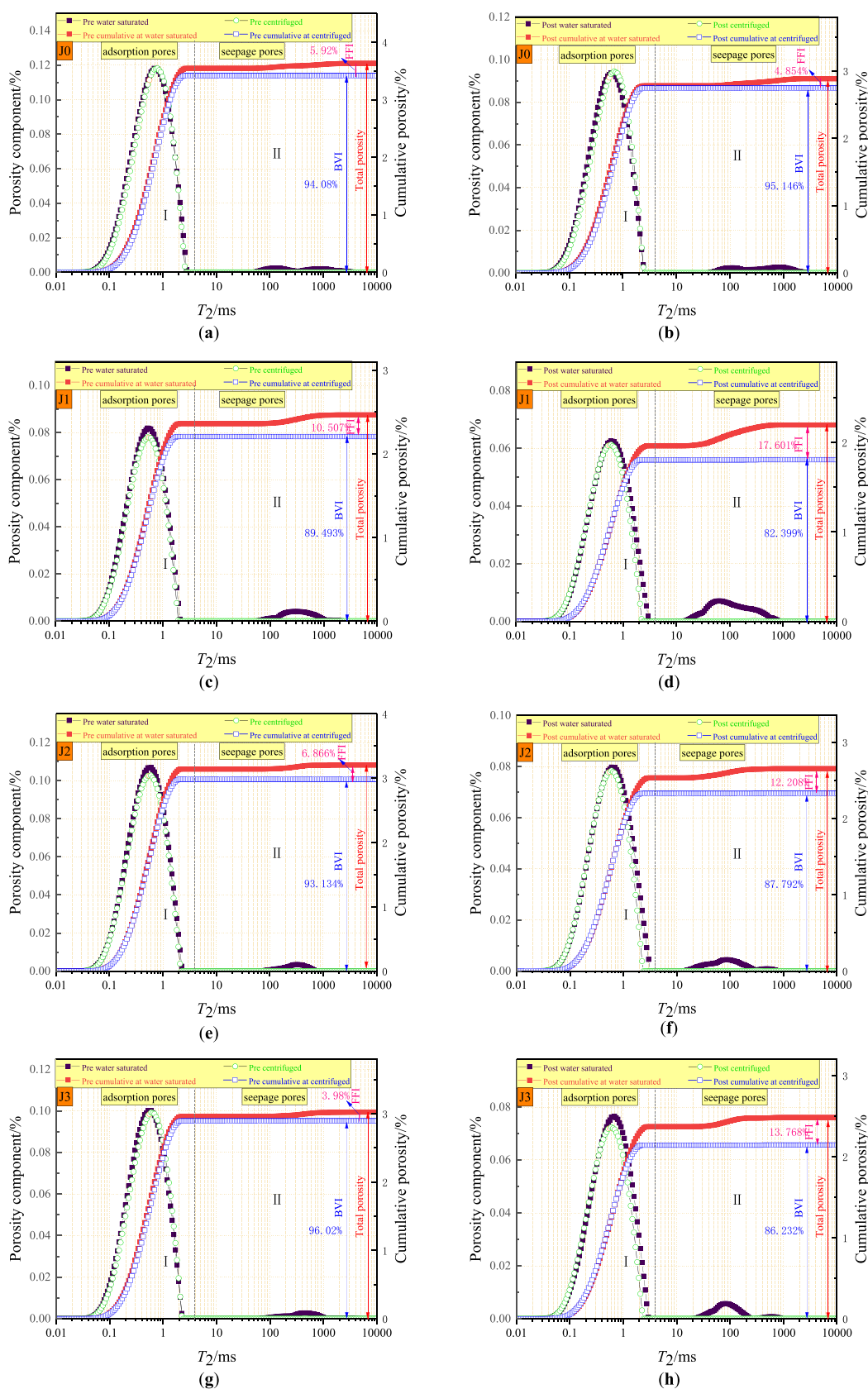
3.2.2. Saturation Change of Movable Fluid. According to the theory of seepage mechanics, when the pore radius in the reservoir decreases to a certain extent, the fluid in the pore will be confined by capillary force or viscous force and remain in an immovable state. The pore size has a critical value on the T_2 spectrum, which is called the T_2 cutoff value of movable fluid. The T_2 cutoff value is an important parameter in the calculation of the saturation of bound fluid. When the T_2 of pore fluid is less than the T_2 cut-off value, the fluid in the pore is called bound fluid or immovable fluid, and the corresponding pore is the adsorption pore. When the T_2 of pore fluid is greater than the T_2 cut-off value, the fluid in the pore is called free fluid or movable fluid, and the corresponding pore is the percolation pore. The volume proportion of bound fluid per pore volume is called bound fluid saturation, and the volume proportion of movable fluid is called movable fluid saturation. Movable fluid saturation can quantitatively characterize reservoir seepage capacity. The higher the movable fluid saturation is, the better the reservoir seepage capacity is. The curves of porosity components and cumulative porosity of the coal sample under saturated and centrifugal conditions before and after treatment by four acid fluids are shown in Figure 5.

As can be seen from Figure 5, the adsorption pores of the saturated porosity component and centrifugal porosity component of the coal sample basically overlapped with each other after distilled water treatment, and the gap between the saturated cumulative porosity and centrifugal cumulative porosity narrowed, indicating that the proportion of movable fluid in the coal sample decreased after distilled water treatment. After acidification, the number of adsorption pores of the centrifugal porosity component of the three coal samples decreased in different degrees compared with the number of adsorption pores of the saturated porosity component. Compared with J1 (Figure 5d) and J2 (Figure 5f), the number of adsorption pores of the centrifugal porosity component of J3 decreased the most compared with that in the saturated porosity component, indicating that the binding

Table 4. Mass of Coal Samples Before and After Acidification Treatment

no. of coal sample	before treatment			after treatment			difference in mass of dry coal sample before and after treatment/g	difference in water content of saturated coal sample before and after treatment/g
	mass of dry coal sample/g	mass of saturated coal sample/g	mass of water in saturated coal sample/g	mass of dry coal sample/g	mass of saturated coal sample/g	mass of water in saturated coal sample/g		
J1	36.12	36.59	0.47	35.31	36.04	0.73	−0.81	0.26
J2	35.70	36.15	0.45	35.26	35.91	0.65	−0.44	0.20
J3	35.99	36.36	0.37	35.57	36.23	0.66	−0.42	0.29

Figure 5. (a) Porosity curve before acid 0 treatment; (b) porosity curve after acid 0 treatment; (c) porosity curve before acid 1 treatment; (d) porosity curve after acid 1 treatment; (e) porosity curve before acid 2 treatment; (f) porosity curve after acid 2 treatment; (g) porosity curve before acid 3 treatment; (h) porosity curve after acid 3 treatment.

capacity of residual water in coal samples decreased to different degrees after acidification, and the that in coal sample J3 decreased most significantly. After acidification, the gap between saturated cumulative porosity and centrifugal cumulative porosity increased for the three coal samples, where the increase amplitude of J3 was the largest, indicating that the proportion of movable fluid in the coal sample increased after acidification. This means that the dissolution effect of acid enlarged the pore size of adsorption pores and transformed it into seepage pores and made them interconnected and develop into a perfect pore network, resulting in a decrease in the pore proportion of adsorption pores and an increase in the pore proportion of seepage pores, which further indicates that acidification has good permeability improvement effect and can effectively improve the gas extraction rate.[22]

In order to eliminate the difference in the initial values of coal samples, it is particularly important to analyze the variation of movable fluid saturation before and after acidification of coal samples. The comparative analysis of the variation of mobile fluid saturation before and after acidification can better meet the requirements of acidification and permeability improvement of the coal bed and improvement of gas production and transport efficiency, which is conducive to exploring the influence of different acid fluids on the permeability improvement effect of the coal sample, so as to realize the selection of optimal mixed acid fluid. Table 5 shows

Table 5. Variation of Movable Fluid Saturation (FFI) before and after Acidification

no. of coal sample	fluid saturation before treatment/%		fluid saturation after treatment/%		absolute change in FFI/%	relative change in FFI/%
	bound fluid (BVI)	movable fluid (FFI)	bound fluid (BVI)	movable fluid (FFI)		
J0	94.08	5.92	95.15	4.85	−1.07	−18.01
J1	89.49	10.51	82.40	17.60	7.09	67.52
J2	93.13	6.87	87.79	12.21	5.34	77.80
J3	96.02	3.98	86.23	13.77	9.79	245.93

the bound fluid saturation and movable fluid saturation of coal samples before and after acidification that are calculated according to saturated porosity and centrifugal porosity.

It can be seen from Table 5 and Figure 5 that the movable fluid saturation of the coal sample after soaking in distilled water decreased from 5.92 to 4.85%, with a decrease rate of 1.07% or a decreased amplitude of 18.01%, indicating that the seepage capacity of the coal after soaking in distilled water decreased. The movable fluid saturation of coal samples after acidification was improved to varying degrees. The movable fluid saturations of J1, J2, and J3 increased from 10.51, 6.87, and 3.98% to 17.60, 12.21, and 13.77%, with increase rates of 7.09, 5.34, and 9.79% or increased amplitudes of 67.52, 77.80, and 245.93%, respectively, indicating that the seepage capacity of the coal sample after acidification was enhanced, and the seepage capacity of J3 was enhanced the most significantly. Although the difference in absolute variation of movable fluid saturation of J1 and J3 before and after acidification was not significant, the absolute variation of the latter was 1.38 times that of the former, but the relative variation of the latter was 3.64 times that of the former. This may be because the initial movable fluid saturation of the coal sample J3 was extremely low, while the absolute and relative changes of movable fluid

saturation of the coal sample in this paper were calculated based on the movable fluid saturation of each coal sample before acidification. In terms of the increased amplitude of movable fluid saturation, J3 acidified by 12%HCl +3%HF exhibited the largest increased amplitude in movable fluid saturation, indicating that the permeability improvement effect of 12%HCL + 3%HF acidification was better than that of 8% HCL + 7%HBF$_4$ and 12%H$_3$PO$_4$ + 3%HF for the Jiulishan coal mine in the Jiaozuo mining area, which is consistent with the previous conclusion that the effective porosity of coal samples increases after acidification.

3.3. Analysis of Variation of Pore Size Distribution.
Coalbed methane mainly exists in the adsorption state in micropores with a large specific surface area, and mesopores and macropores are the main channels for gas diffusion and seepage. Therefore, studying the pore size distribution of coal after acidification is of great theoretical significance for analyzing the characteristics of gas migration after acidification. According to previous studies, pore size is divided into three types, micropores (pore size <0.01 μm), mesopores (0.01 μm < pore size<0.1 μm), macropores (0.1 μm < pore size < 100 μm).[36,37] The purpose of acidizing antireflection operation during CBM extraction is to reduce the number of micropores and increase the number of meso- and macropores, thus promoting gas diffusion and seepage and improving gas extraction efficiency. The pore size distribution tested by LFNMR before and after acidification treatment with different solutions is shown in Figure 6. As can be seen from the pore size distribution of coal samples treated with different solutions in Figure 6, the pore size distribution curve of the coal sample J0 treated with distilled water shifts to the left, indicating that the pore size of J0 decreases and the number of pores with smaller pore size increases. The pore size distribution curves of J1, J2, and J3 after acidification are shifted to the right, indicating that acidification increases the pore size of micropores in coal samples and the number of pores with larger pore sizes, and the pore sizes of mesopores and macropores increase to varying degrees, which is consistent with the conclusion of T_2 spectrum analysis by LFNMR. Compared with the J1 and J2 samples treated with 8%HCL + 7%HBF$_4$ and 12% H$_3$PO$_4$ + 3%HF, the pore sizes of the mesopore and macropore in the coal sample J3 treated with 12%HCL + 3%HF increase more significantly, and channels for gas diffusion and seepage migration in the coal sample are increased, which is beneficial to gas extraction.

3.4. Analysis of Variation of Pore-Throat Distribution.
The pore system is basically a pore network composed of small pore-throat units. Pore-throat is a narrow throat connecting pores. The size of pore-throat determines the connectivity between pores, affects the difficulty in gas transport in the cracks of coal bed, and thus affects the gas extraction rate. Therefore, studying the variation of pore-throat distribution characteristics before and after acidification is of great significance to the evaluation of acidification technology on enhancing gas extraction. LFNMR core measurement software was used to measure pore-throat distribution characteristics of coal samples before and after soaking in four acid fluids, and the results are shown in Figure 7.

According to the pore classification criteria proposed by predecessors,[38−40] pore throats smaller than 0.1 μm are considered as adsorption pores, and pore throats larger than 0.1 μm are considered as seepage pores. The adsorption pore is the main adsorption and storage space of gas, which mainly
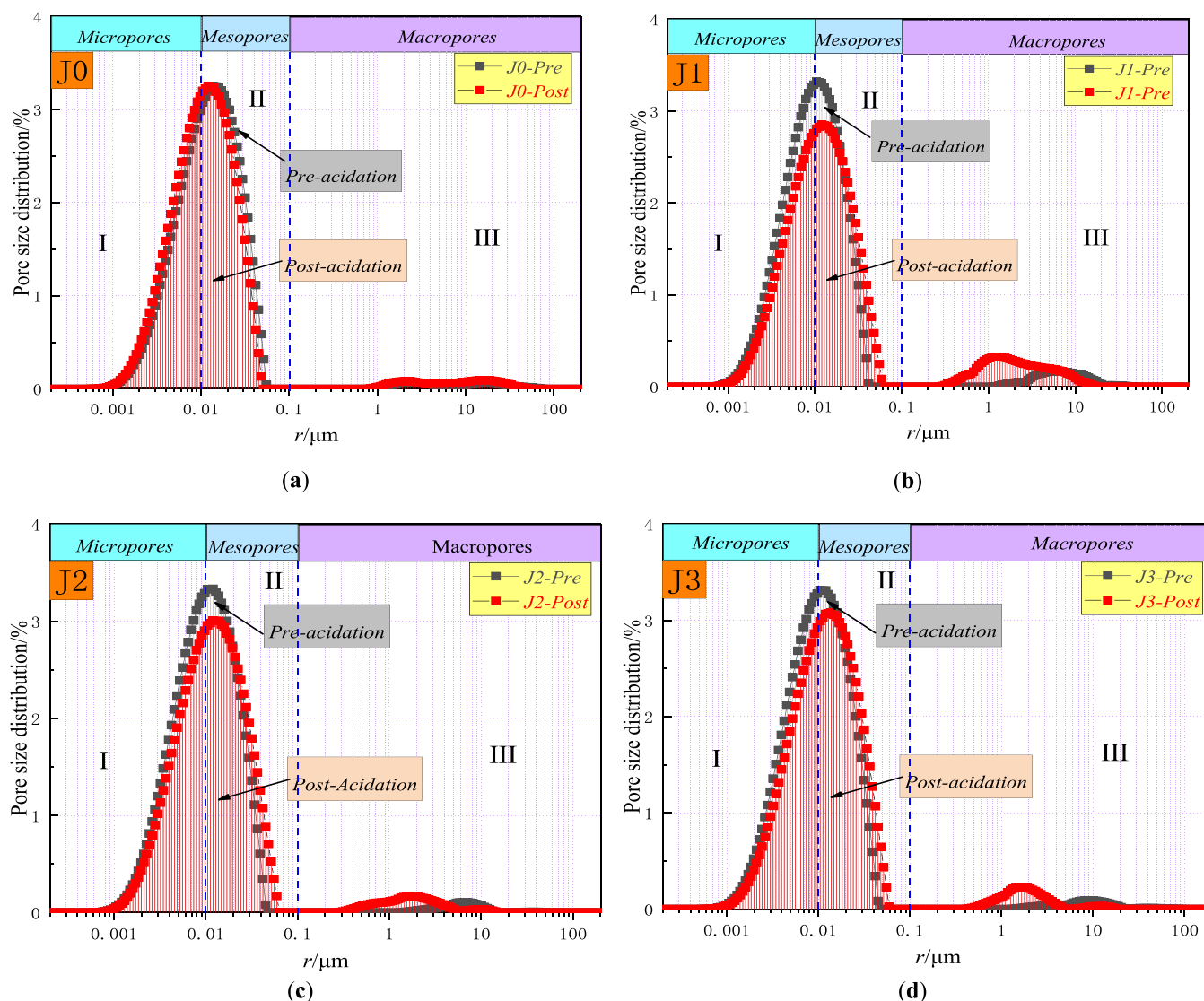
Figure 6. (a) Comparison of pore size distribution before and after treatment of acid 0; (b) comparison of pore size distribution before and after treatment of acid 1; (c) comparison of pore size distribution before and after treatment of acid 2; (d) comparison of pore size distribution before and after treatment of acid 3.

affects the adsorption and desorption of gas,[41,42] while the seepage pore is the channel of gas diffusion and seepage, and its development degree mainly affects the ability of gas diffusion and seepage.

It can be seen from Figure 7 that adsorption pores were dominant in all coal samples before and after treatment, but the proportion of adsorption pores decreased and the proportion of seepage pores increased after acidification, and the proportion of seepage pore-throats in J1, J2 ,and J3 after acidification increased by 2.44, 2.56, and 6.33%, respectively. Combined with Figure 7d, it can be seen that compared with the variation of pore-throat distribution characteristics of J1 and J2, the pore-throat range of seepage pores in J3 treated with 12%HCL + 3%HF was the widest, and the number of pore-throats with a pore size ranging from 0.4 to 10 μm increased most significantly compared with that before acidification. The results show that during acidification and permeability improvement operation, 12%HCL + 3%HF can best meet the requirements of increasing the number of seepage pores, enhancing the connectivity between pores,

promoting gas diffusion and seepage, and finally improving the gas extraction rate.

3.5. Analysis of Permeability Variation. The changes of coal porosity, mobile fluid saturation, and pore-throat distribution are macroscopically expressed as the change of permeability. Permeability reflects the ability of coal bed to produce gas and allow gas flow, so it can be used as the final parameter to evaluate the effect of acidification and permeability improvement. Based on the NMR porosity, movable fluid saturation, and bound fluid saturation measured by LFNMR instrument, formula 4 was used to calculate the nuclear magnetic permeability and its variation of coal samples before and after acidification, and the results are shown in Table 6.

As can be seen from Table 6, the permeability of coal sample J0 after soaking in distilled water decreased from 0.04 to 0.01 mD, with a decrease rate of 0.03 mD or a decreased amplitude of 74.42%. The reason may be that the clay minerals in coal expanded when they met water, which reduced the space of pores and fissures in coal, blocked the pore-throat channels,
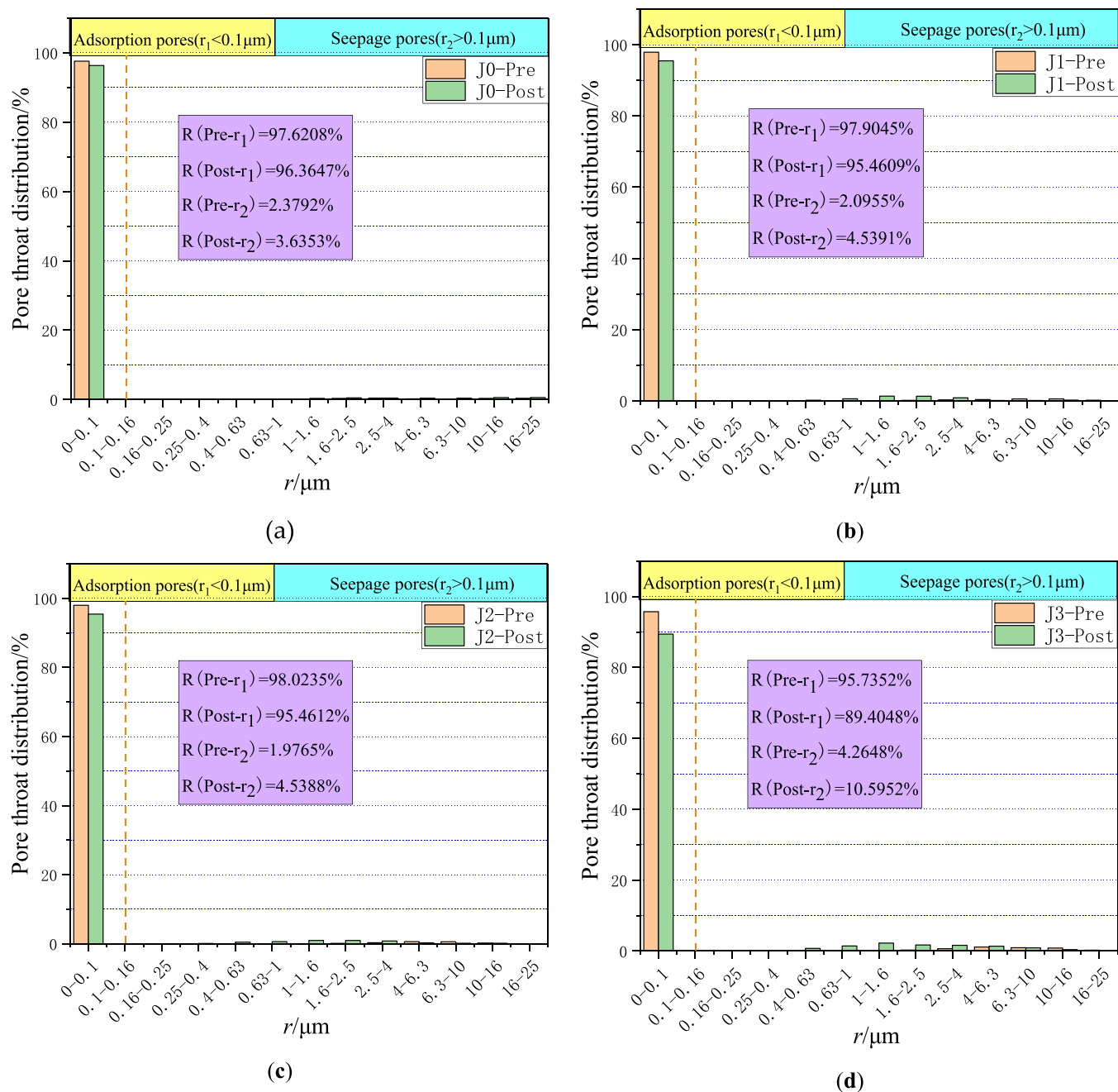
Figure 7. (a) Pore-throat distribution curve before and after acid 0 treatment; (b) pore-throat distribution curve before and after acid 1 treatment; (c) pore-throat distribution curve before and after acid 2 treatment; (d) pore-throat distribution curve before and after acid 3 treatment.

Table 6. Permeability and its Variation Before and After Acidification

no. of coal sample	permeability before treatment/ mD	permeability after treatment/ mD	absolute change in permeability/ mD	relative change in permeability/%
J0	0.04	0.01	−0.03	−74.42
J1	0.03	0.07	0.03	106.25
J2	0.04	0.06	0.02	66.66
J3	0.01	0.06	0.05	577.77

and reduced the connectivity between pores and fissures in coal, leading to a significant decline in permeability of coal. This is also the reason why permeability decreased rather than increased when adopting hydraulic operation to enhance the permeability of the coal bed. After acidification treatment, the nuclear magnetic permeability of each coal sample increased to different degrees. The permeability of J1, J2, and J3 increased from 0.03, 0.04, and 0.01 mD to 0.07, 0.06, and 0.06 mD, with increments of 0.03, 0.02, and 0.05 mD and increase rates of 106.25, 66.66, and 577.77%, respectively. It can be seen that the permeability of J3 acidified by 12%HCl +3%HF increased the most, indicating that 12%HCl +3%HF acidification can significantly improve the permeability of high-rank coal in the Jiulishan coal mine. Although the absolute change of permeability of J1 and J3 coal samples before and after acidification was not significant, where the latter was 1.53 times of the former, the relative change of the latter was 5.44 times of

Table 7. Dissolution Rate (%)

no. of coal sample	J1			J2			J3		
mass of coal	m_1	m_2	m_3	m_1	m_2	m_3	m_1	m_2	m_3
sample/g	3.01	4.49	1.56	3.01	4.50	1.56	3.01	4.49	1.56
dissolution rate/%		2.6			2.24			2.71	

the former. The reason may be that the absolute change and relative change of permeability of the coal sample in this paper were calculated based on the initial permeability of each coal sample before acidification, and the initial permeability of coal sample J3 was very low. It shows that the permeability improvement effect of 12%HCL + 3%HF was better than that of 8%HCL + 7%HBF$_4$ and 12%H$_3$PO$_4$ + 3%HF for the Jiulishan coal mine in the Jiaozuo mining area. The variation law of nuclear magnetic permeability of coal samples was consistent with the variation law of porosity, movable fluid saturation, and pore-throat distribution. Therefore, the author believes that mixed acid 12%HCL + 3%HF has the best permeability improvement effect on high-rank coal in the Jiulishan coal mine, and it can be used as the optimal acid system for implementing acidification and permeability improvement technology in Jiulishan coal mine in the Jiaozuo mining area.

3.6. Results and Analysis of Static Dissolution Test.

Calculating the dissolution rate of coal samples before and after acidification by acid dissolution experiment is a basic method for quantitative evaluation of acid rock reaction characteristics, which can be easily operated. The dissolution rate is one of the main parameters evaluating the acidification and permeability improvement effects of the coal bed, which can quantitatively characterize the dissolution ability of acid to coal. The higher the dissolution rate is, the stronger the dissolution ability of acid to coal is, and the better the acidification and permeability improvement effect is. Table 7 shows the dissolution rates of three acidified coal samples calculated according to eq 4.

According to Table 7, the dissolution rates of J1, J2, and J3 acidized by 8%HCL + 7%HBF$_4$, 12%H$_3$PO$_4$ + 3%HF, and 12% HCL + 3%HF were 2.6, 2.24, and 2.71%, respectively. It can be seen that the dissolution rate of J3 was the highest, followed by that of J1, and that of J2 was the lowest, indicating that the dissolution capacity of 12%HCL + 3%HF was better than that of 8%HCL + 7%HBF$_4$ and 12%H$_3$PO$_4$ + 3%HF for the Jiulishan coal mine, that is, the acidification and permeability improvement effect of 12%HCl +3%HF was the best. The results of the dissolution rate were consistent with the results of effective porosity, movable fluid saturation, and permeability analysis, which further confirms that 12%HCL + 3%HF is the optimal mixed acid fluid suitable for acidification and permeability improvement of high-rank coal in the Jiulishan coal mine in the Jiaozuo mining area.

4. CONCLUSIONS

(1) After acidification, the volume proportion of the micropore in coal decreased significantly, the number and volume proportion of the mesopore and macropore-microcrack increased significantly, and the connectivity between the mesopore and macropore-microcrack was enhanced. Compared with the coal sample J2, the number and volume proportion of the mesopore and macropore-microcrack of J1 and J3 after acidification

increased more significantly, and the connectivity between pores was better for the two coal samples. After distilled water treatment, the pore size, number, and volume of the micropore, mesopore, and macropore-microcrack in coal samples all decreased.

(2) After acidification, the proportion of adsorption pores decreased, while that of seepage pores increased. After acidification, the proportions of pore-throats of seepage pores of J1, J2, and J3 increased by 2.44, 2.56, and 6.33%, respectively. Compared with the variation of pore-throat distribution characteristics of J1 and J2, the pore-throat variation range of the seepage pore of J3 treated with 12%HCL + 3%HF was the widest, and the number of pore-throats with a pore size ranging from 0.4 to 10 μm increased the most significantly compared with that before acidification.

(3) After distilled water treatment, effective porosity, movable fluid saturation, and nuclear magnetic permeability of the coal sample J0 decreased. After acidification, the effective porosities of J1, J2, and J3 increased by 0.13, 0.10, and 0.22%, respectively, movable fluid saturations increased by 7.09, 5.34, and 9.79%, respectively, and nuclear magnetic permeabilities increased by 0.03, 0.02, and 0.05 mD, respectively. The increases in effective porosity, movable fluid saturation, and nuclear magnetic permeability of J3 acidified by 12% HCL + 3%HF were the most significant. For the high-rank coal of the Jiulishan coal mine in the Jiaozuo mining area, 12%HCL + 3%HF as a mixed acid fluid had the strongest ability to improve the pore structure of coal and exhibited the best effect of acidification and permeability improvement, so it can be used as the optimal acid system for implementing acidification and permeability improvement technology in the Jiulishan coal mine of the Jiaozuo mining area.

■ AUTHOR INFORMATION

Corresponding Author

Xuebo Zhang − College of Safety Science and Engineering, Henan Polytechnic University, Jiaozuo, Henan 454003, China; ● orcid.org/0000-0002-4211-8758; Email: zhxb@hpu.edu.cn

Authors

Chunxia Wang − College of Safety Science and Engineering, Henan Polytechnic University, Jiaozuo, Henan 454003, China; School of Mining and Mechanical Engineering, Liupanshui Normal University, Liupanshui, Guizhou 553004, China; ● orcid.org/0000-0002-8962-8253

Jianliang Gao − College of Safety Science and Engineering, Henan Polytechnic University, Jiaozuo, Henan 454003, China

Complete contact information is available at:
https://pubs.acs.org/10.1021/acsomega.2c03810

Author Contributions

C.W. conceived the experiment, analyzed the results, and drafted the manuscript; J.G., X.Z. coordinated the study and helped draft the manuscript. All authors gave final approval for publication.

Notes

The authors declare no competing financial interest.

■ REFERENCES

(1) Pillalamarry, M.; Harpalani, S.; Liu, S. Gas diffusion behavior of coal and its impact on production from coalbed methane reservoirs. *Int. J. Coal Geol.* **2011**, *86*, 342−348.

(2) Zhao, B.; Wen, G.; Sun, H.; Zhao, X. Experimental study of the pore structure and permeability of coal by acidizing. *Energies* **2018**, *11*, 1162.

(3) Liu, Q.; Cheng, Y.; Wang, H.; Zhou, H.; Wang, L.; Li, W.; Liu, H. Numerical assessment of the effect of equilibration time on coal permeability evolution characteristics. *Fuel* **2015**, *140*, 81−89.

(4) Li, B.; Zhang, J.; Ding, Z.; Wang, B.; Li, P. A dynamic evolution model of coal permeability during enhanced coalbed methane recovery by N2 injection: experimental observations and numerical simulation. *RSC Adv.* **2021**, *11*, 17249−17258.

(5) Song, S.-B.; Liu, J.-F.; Yang, D.-S.; Ni, H.-Y.; Huang, B.-X.; Zhang, K.; Mao, X.-B. Pore structure characterization and permeability prediction of coal samples based on SEM images. *J. Nat. Gas Sci. Eng.* **2019**, *67*, 160−171.

(6) Chu, Y.; Sun, H.; Zhang, D.; Yu, G. Nuclear magnetic resonance study of the influence of the liquid nitrogen freeze-thaw process on the pore structure of anthracite coal. *Energy Sci. Eng.* **2020**, *8*, 1681−1692.

(7) Hou, P.; Gao, F.; Ju, Y.; Cheng, H.; Gao, Y.; Xue, Y.; Yang, Y. Changes in pore structure and permeability of low permeability coal under pulse gas fracturing. *J. Nat. Gas Sci. Eng.* **2016**, *34*, 1017−1026.

(8) Zhang, J.; Li, B.; Liu, Y.; Li, P.; Fu, J.; Chen, L.; Ding, P. Dynamic multifield coupling model of gas drainage and a new remedy method for borehole leakage. *Acta Geotechnica* **2022**, 1−17.

(9) Liu, J.; Hu, J.; Jia, G.; Gao, J.; Wang, D. Nuclear magnetic resonance study on microstructure and permeability of coals of different ranks. *Adv. Civ. Eng.* **2020**, 1−10.

(10) Li, B.; Shi, Z.; Li, L.; Zhang, J.; Huang, L.; He, Y. Simulation study on the deflection and expansion of hydraulic fractures in coal-rock complexes. *Energy Rep.* **2022**, *8*, 9958−9968.

(11) Li, Z.; Liu, D.; Cai, Y.; Wang, Y.; Si, G. Evaluation of coal petrophysics incorporating fractal characteristics by mercury intrusion porosimetry and low-field NMR. *Fuel* **2020**, *263*, No. 116802.

(12) Li, X.; Kang, Y. Effect of fracturing fluid immersion on methane adsorption/desorption of coal. *J. Nat. Gas Sci. Eng.* **2016**, *34*, 449−457.

(13) Huang, W.; Lei, M.; Qiu, Z.; Leong, Y.-K.; Zhong, H.; Zhang, S. Damage mechanism and protection measures of a coalbed methane reservoir in the Zhengzhuang block. *J. Nat. Gas Sci. Eng.* **2015**, *26*, 683−694.

(14) Liu, Z.; Liu, D.; Cai, Y.; Qiu, Y. Permeability, mineral and pore characteristics of coals response to acid treatment by NMR and QEMSCAN: Insights into acid sensitivity mechanism. *J. Pet. Sci. Eng.* **2021**, *198*, No. 108205.

(15) Finkelman, R. B.; Dai, S.; French, D. The importance of minerals in coal as the hosts of chemical elements:A review. *Int. J. Coal Geol.* **2019**, *212*, No. 103251.

(16) Dai, S.; Li, T.; Jiang, Y.; Ward, C. R.; Hower, J. C.; Sun, J.; Liu, J.; Song, H.; Wei, J.; Li, Q.; Xie, P.; Huang, Q. Mineralogical and geochemical compositions of the Pennsylvanian coal in the Hailiushu Mine, Daqingshan Coalfield, Inner Mongolia, China: Implications of sediment-source region and acid hydrothermal solutions. *Int. J. Coal Geol.* **2015**, *137*, 92−110.

(17) Steel, K. M.; Besida, J.; O'Donnell, T. A.; Wood, D. G. Production of Ultra Clean Coal:Part II-Ionic equilibria in solution when mineral matter from black coal is treated with aqueous hydrofluoric acid. *Fuel Process. Technol.* **2001**, *70*, 193−219.

(18) Steel, K. M.; Patrick, J. W. The production of ultra clean coal by sequential leaching with HF followed by HNO_3. *Fuel* **2003**, *82*, 1917−1920.

(19) Zhang, L.; Li, Z.; Yang, Y.; Zhou, Y.; Kong, B.; Li, J.; Si, L. Effect of acid treatment on the characteristics and structures of high-sulfur bituminous coal. *Fuel* **2016**, *184*, 418−429.

(20) Yang, H.; Yu, Y.; Cheng, W.; Rui, J.; Xu, Q. Influence of acetic acid dissolution time on evolution of coal phase and surface morphology. *Fuel* **2021**, *286*, No. 119464.

(21) Yu, Y.; Yang, H.; Cheng, W.; Gao, C.; Zheng, L.; Xin, Q. Effect of acetic acid concentration on functional group and microcrystalline structure of bituminous coal. *Fuel* **2021**, *288*, No. 119711.

(22) Xie, H.; Ni, G.; Li, S.; Sun, Q.; Dong, K.; Xie, J.; Wang, G.; Liu, Y. The influence of surfactant on pore fractal characteristics of composite acidized coal. *Fuel* **2019**, *253*, 741−753.

(23) Ni, G.; Xie, H.; Li, S.; Sun, Q.; Huang, D.; Cheng, Y.; Wang, N. The effect of anionic surfactant (SDS) on pore-fracture evolution of acidified coal and its significance for coalbed methane extraction. *Adv. Powder Technol.* **2019**, *30*, 940−951.

(24) Balucan, R. D.; Turner, L. G.; Steel, K. M. Acid-induced mineral alteration and its influence on the permeability and compressibility of coal. *J. Nat. Gas Sci. Eng.* **2016**, *33*, 973−987.

(25) Balucan, R. D.; Turner, L. G.; Steel, K. M. X-ray μCT investigations of the effects of cleat demineralization by HCL acidizing on coal permeability. *J. Nat. Gas Sci. Eng.* **2018**, *55*, 206−218.

(26) Ramandi, H. L.; Liu, M.; Tadbiri, S.; Mostaghimi, P. Impact of dissolution of syngenetic and epigenetic minerals on coal permeability. *Chem. Geol.* **2018**, *486*, 31−39.

(27) Cai, Y.; Liu, D.; Pan, Z.; Yao, Y.; Li, J.; Qiu, Y. Petrophysical characterization of Chinese coal cores with heat treatment by nuclear magnetic resonance. *Fuel* **2013**, *108*, 292−302.

(28) Jin, H.; Nie, W.; Zhang, H.; Liu, Y.; Bao, Q.; Wang, H.; Huang, D. Preparation and characterization of a novel environmentally friendly coal dust suppressant. *J. Appl. Polym. Sci.* **2019**, *136*, 47354.

(29) Yao, Y.; Liu, D. Comparison of low-field NMR and mercury intrusion porosimetry in characterizing pore size distributions of coals. *Fuel* **2012**, *95*, 152−158.

(30) Zhou, G.; Fan, T.; Xu, M.; Qiu, H.; Wang, J.; Qiu, L. The development and characterization of a novel coagulant for dust suppression in open-cast coal mines. *Adsorpt. Sci. Technol.* **2018**, *36*, 608−624.

(31) Li, S.; Luo, M. K.; Fan, C. J.; Bi, H. J.; Ren, Y. P. Quantitative characterization of the effect of acidification in coals by NMR and Low-temperature nitrogen adsorption. *J. China Coal Soc.* **2017**, *42*, 1748−1756.

(32) Liu, L.; Yang, M.; Zhang, X.; Mao, J.; Chai, P. LNMR experimental study on the influence of gas pressure on methane adsorption law of middle-rank coal. *J. Nat. Gas Sci. Eng.* **2021**, *91*, No. 103949.

(33) Yao, Y.; Liu, J.; Liu, D.; Chen, J.; Pan, Z. A new application of NMR in characterization of multiphase methane and adsorption capacity of shale. *Int. J. Coal Geol.* **2019**, *201*, 76−85.

(34) Li, R.; Wang, K.; Wang, Y.-J. Indoor study on acidification for enhancing the permeability of coal. *J. China Coal Soc.* **2014**, *39*, 913−917.

(35) Zhao, W.; Li, R.; Wu, X.; Tang, J.; Wang, K.; Wang, Y. Preliminary indoor experiments on enhancing permeability rate of coal reservoir by using acidification technology. *China Coalbed Methane* **2012**, *9*, 10−13.

(36) Zhang, Q.; Hu, X.-M.; Wu, M.-Y.; Zhao, Y.-Y.; Yu, C. Effects of different catalysts on the structure and properties of polyurethane/water glass grouting materials. *J. Appl. Polym. Sci.* **2018**, *135*, 46460.

(37) Liu, Q.; Nie, W.; Hua, Y.; Peng, H.; Liu, C.; Wei, C. Research on tunnel ventilation systems:Dust Diffusion and Pollution Behaviour by air curtains based on CFD technology and field measurement. *Build. Environ.* **2019**, *147*, 444−460.

(38) Liu, Z.; Yang, H.; Wang, W.; Cheng, W.; Xin, L. Experimental study on the pore structure fractals and seepage characteristics of a coal sample around a borehole in coal seam water infusion. *Transp. Porous Media* **2018**, *125*, 289−309.

(39) Liu, Y.; Nie, W.; Jin, H.; Ma, H.; Hua, Y.; Cai, P.; Wei, W. Solidifying dust suppressant based on modified chitosan and experimental study on its dust suppression performance. *Adsorpt. Sci. Technol.* **2018**, *36*, 640−654.

(40) Ni, G.; Dong, K.; Li, S.; Sun, Q. Gas desorption characteristics effected by the pulsating hydraulic fracturing in coal. *Fuel* **2019**, *236*, 190−200.

(41) Tao, S.; Chen, S.; Pan, Z. Current status, challenges, and policy suggestions for coalbed methane industry development in China: A review. *Energy Sci. Eng.* **2019**, 1059−1074.

(42) Tao, S.; Pan, Z.; Tang, S.; Chen, S. Current status and geological conditions for the applicability of CBM drilling technologies in China:A review. *Int. J. Coal Geol.* **2019**, *202*, 95−108.